Cytoplasmic-translocated Ku70 senses intracellular DNA and mediates interferon-lambda1 induction

Hongyan Sui*, (iD) Qian Chen and Tomozumi Imamichi*, (iD)

Laboratory of Human Retrovirology and Immunoinformatics, Frederick National Laboratory for Cancer Research, Frederick, MD, USA

Summary

We have previously identified that human Ku70, a nuclear protein, serves as a cytosolic DNA sensor. Upon transfection with DNA or infection with DNA virus, Ku70 translocates from the nucleus into the cytoplasm and then predominately induces interferon lambda1 (IFN-λ1) rather than IFN-alpha or IFN-beta, through a STING-dependent signalling pathway. However, a detailed mechanism for Ku70 cytoplasmic translocation and its correlation with IFN-λ1 induction have not been fully elucidated. Here, we observed that cytoplasmic translocation of Ku70 only occurred in DNA-triggered IFN-λ1-inducible cells. Additionally, infection by Herpes simplex virus type-1 (HSV-1), a DNA virus, induces cytoplasmic translocation of Ku70 and IFN-λ1 induction in a strain-dependent manner: the translocation and IFN-λ1 induction were detected upon infection by HSV-1 McKrae, but not MacIntyre, strain. A kinetic analysis indicated that cytoplasmic translocation of Ku70 was initiated right after DNA transfection and was peaked at 6 hr after DNA stimulation. Furthermore, treatment with leptomycin B, a nuclear export inhibitor, inhibited both Ku70 translocation and IFN-λ1 induction, suggesting that Ku70 translocation is an essential and early event for its cytosolic DNA sensing. We further confirmed that enhancing the acetylation status of the cells promotes Ku70's cytoplasmic accumulation, and therefore increases DNA-mediated IFN-λ1 induction. These findings provide insights into the molecular mechanism by which the versatile sensor detects pathogenic DNA in a localization-dependent manner.

Keywords: acetylation; cytosolic DNA sensor; IFN-λ1; Ku70; translocation.

Introduction

Recognition of nucleic acid (DNA or RNA) pathogen is essential for initiating innate immune responses, which are induced by a series of pattern recognition receptors (PRRs).[1] DNA represents a potent pathogen-associated molecular patterns (PAMPs) that stimulates interferon (IFN) responses in many cell types.[2–6] Approximately 10 intracellular DNA sensors have been identified, such as Z-DNA binding protein 1 (DAI, ZBP1),[7] RNA polymerase III (Pol III),[8] IFN-γ-inducible factor 16 (IFI16),[9] DExD/H-box helicase 41(DDX41),[10] cyclic GMP-AMP synthase (cGAS)[11,12] and Ku70.[13,14]

Ku70 forms a heterodimer with Ku80 in the nucleus[15] that is required for non-homologous end-joining DNA repair, VDJ recombination of immunoglobulin,

---

telomerase maintenance and various other nuclear processes.[16,17] In addition to its biological functions in the nucleus, Ku70 also suppresses Bax-mediated apoptosis in cytoplasm.[18–21] We have previously reported that Ku70 serves as a cytosolic DNA sensor in primary human cells that detects single- and double-stranded DNA and predominantly produces IFN-λ1, a type III IFN. This induction is mediated via a STING-dependent signalling pathway, involving the activation of IFN regulatory factor (IRF)-3, IRF-1 and IRF-7.[13,14] Ferguson *et al.*[22] revealed that the DNA-PK complex containing Ku70/Ku80 plays a role as a DNA sensor that triggers IRF3-dependent IFN-beta (IFN-β) production. Li *et al.*[23] reported that Ku sensed hepatitis B virus DNA and induced chemokine secretion mediated by IRF1 in liver-derived cells. More recently, Wang et al. reported that Ku70 is involved in suppression of HTLV-1 infection by inducing type-I IFN in multiple cell types.[24]

The active import of translated proteins into the nucleus requires the presence of a nuclear localization sequence (NLS),[25] and Ku70 possesses an NLS domain in the molecule. The various NLS sequences are identified and classified mainly into two groups: (1) a single cluster of basic amino acids such as the NLS of the SV40 T-antigen (2) and a bipartite type in which two sets of adjacent basic amino acids are separated by a stretch of approximately 10 amino acids.[26] A process of the NLS-dependent nuclear import requires at least four proteins that act sequentially with NLS-containing proteins. First, the NLS domain of the transporting protein needs to bind with the NLS receptors, such as importin-α (Impα) and then forms a complex with importin-β (Impβ). After that, the complex will target nuclear pore proteins followed by Ran-mediated ATP/GTP-dependent translocation through the nuclear pore.[27,28] The NLS of Ku70 is a variant of the bipartite type and highly conserved among different species. The Ku70 NLS is recognized by the two components of the nuclear targeting complex, PTAC58 and PTAC97, but not by either PTAC58 or PTAC97 alone.[29]

We have previously reported that Ku70 undergoes a translocation from the nucleus to the cytoplasm upon transfection with DNA or infection with DNA virus, and then, Ku70 forms a complex with DNA followed by binding to STING and activates downstream signalling.[13] This Ku70-mediated IFN-λ1 induction is a predominant response in HEK293 cells, THP-1 cells and primary human macrophage. IFN-α and IFN-β were also simultaneously induced, but the amount of produced protein was significantly lower than IFN-λ1.[13] The purpose of the current study was to further clarify Ku70's cytoplasmic translocation in details and its correlation with IFN-λ1 induction.

In the current study, we demonstrate that Ku70 translocation from the nucleus to the cytoplasm is an early and required event for Ku70 to act as a DNA sensor in initiating innate immune response. We also confirm that acetylation at NLS of Ku70 is 'a toggle switch' for localization of Ku70 in the nucleus or the cytoplasm, and therefore, the acetylation modulates cytosolic DNA via Ku70-mediated IFN-λ1 innate immune response. Our findings provide additional information regarding the molecular mechanism of the DNA or DNA virus via Ku70-mediated innate immune response. It also advances our understanding of innate immune response and expands the current repertoire of DNA-sensing mechanisms.

Materials and methods

Cells, viruses and antibodies

Human embryonic kidney 293 (HEK293), human cervical cancer (HeLa), human rhabdomyosarcoma (RD) and SV40 T-antigen-transformed HEK293 (293T) were obtained from American Type Culture Collection (ATCC, Rockville, MD) and maintained following the manufacturer's instructions. HSV-1 virus strain MacIntyre was obtained from Advanced Biotechnologies Inc. (Eldersburg, MD), and HSV-1 virus strain McKrae was kindly provided from Dr. Jeffrey I. Cohen (NIAID/NIH, Bethesda). Virus stock was prepared using Vero cells (ATCC), and virus titre was determined by plaque-forming assay.[30] Antibodies used in this study are listed in Table S1, and the clone details and supplier's catalog number are provided.

DNA labelling and DNA transfection

As a DNA stimulant, a linearized DNA was prepared by digesting a PCR cloning vector, pCR2·1 plasmid (Thermo Fisher Scientific, Waltham, MA), as previously described.[13] For immunofluorescence staining, the linearized DNA was labelled with Label IT® MFP488 (Mirus, Madison, WI) following the manufacturer's instructions. Non-labelled DNA or labelled DNA were transfected using Lipofectamine 2000 (Thermo Fisher Scientific) for HeLa or RD cells and Transit 293 (Mirus) for HEK293 or HEK293T cells.

Plasmid construction

The pCR2·1 plasmid (Thermo Fisher Scientific) was digested with *EcoR*I followed by purification using a PCR purification kit (Qiagen, Germantown, MD), and this digested plasmid was used as a non-coding DNA stimulant as previously described.[13,14] A C-terminal FLAG-tagged Ku70 expression vector (Ku70 WT) was constructed as follows: Ku70 cDNA was synthesized from 5 μg total cellular RNA of HEK cells using a Superscript First-Stand Synthesis System for reverse transcriptase–

polymerase chain reaction (RT-PCR) (Thermo Fisher Scientific) and then followed by a PCR amplification using a forward primer: 5′-GAATCGATGCGCATGCGTG-GATTGTCGTCTTCTG-3′ and a reverse primer: 5′-CCGGATCCGTCCTGGAAGTGCTTGGTGAGGGCTTC-CAG-3′. A mutant Ku70 with acetylation-mimicking double mutations at NLS codons 553 and 556 of Ku70 (Ku70 MT) was constructed using a QuikChange II Site-Directed Mutagenesis Kit (Agilent, Santa Clara, CA) with a sense primer 5′-GATAATGAAGGTTCTGGAAGC-CAAAGGCCCCAGGTGGAGTATTCAGAAGAG-3′ and a corresponding antisense primer. The PCR product for Ku70 WT or Ku70 MT was cloned into pCMV5a (Sigma-Aldrich, St. Louis, MO). The insertion was confirmed by DNA sequencing with Big Dye version 3.0 (Thermo Fisher Scientific) on SeqStudio Genetic Analyzer (Thermo Fisher Scientific).

IFN-λ1 reporter assay

IFN-λ1 reporter assay was performed as previously described.[31] Briefly, 293T cells (30×10^3 cells per well) were seeded in 6-well plates and transfected with 100 ng of pGL4–IFN-λ1, 10 ng of pTK-RL (Promega, Madison, WI) and the appropriate amounts of STING expression vector, wild-type Ku70 expression vector or mutant Ku70 expression vector. The cells were cultured for two days and then stimulated with 1 μg of linearized DNA by transfection. 24 hr after transfection, the cells were collected for the luciferase assay. The luciferase assay was performed with Dual-Glo luciferase assay system reagents (Promega). Relative luciferase activity was calculated based on the ratio of the luminescence of *firefly* luciferase to that of *Renilla* luciferase.

RNA extraction and real-time RT-PCR

Total cellular RNA was isolated from cells using the RNeasy Isolation Kit (Qiagen, Valencia, CA). The cDNA was synthesized from total RNA using TaqMan reverse transcription reagents (Thermo Fisher Scientific) using random hexamer oligos as a primer, according to the manufacturer's instructions. IFN-α, IFN-β, IFN-λ1, IFN-λ2/3 and IFN-λ4 mRNA expression levels were measured using quantitative RT-PCR on a CFX96 real-time system (Bio-Rad, Hercules, CA) as previously described.[31] A two-temperature cycle of 95°C for 15 seconds and 60°C for 1 min (repeated for 40 cycles) was used. Relative quantities of transcripts were calculated with the $\Delta\Delta C_t$ method with *GAPDH* mRNA as a reference. Normalized samples were expressed relative to the average ΔC_t value for controls to obtain relative fold changes in mRNA abundance. All the probes we used for real-time RT-PCR were purchased from Thermo Fisher Scientific, the assay identification number for each probe is listed the Table S2.

Western blot

Whole-cell lysates were prepared using RIPA buffer (Boston Bio Products, Ashland, MA), and cytosolic fraction was extracted using Nuclear Extract Kit (Active Motif, Carlsbad, CA) following a protocol for the isolation of cytosolic fraction. Protein concentrations of the cell lysates were quantified using a BCA protein assay (Thermo Scientific) to ensure equal amounts of total protein were loaded in each well of NuPAGE 4–12% Bis-Tris Gel (Invitrogen). Proteins were transferred onto a nitrocellulose membrane and blotted with the appropriate antibodies, followed by the horseradish peroxidase (HRP)-conjugated secondary antibodies, and the detection was performed using ECL Plus Western Blotting Detection Reagents (GE Healthcare). The intensity of the band was analysed by Fiji–ImageJ.

Immunofluorescence staining and confocal microscopy

Immunofluorescence staining was performed as previously described.[13] Cells grown on 15 mm coverslip-inserted 12-well plates were fixed in 4% paraformaldehyde, blocked in blocking buffer [1× phosphate-buffered saline, 5% normal goat serum (Cell Signaling) and 0·1% saponin (Alfa Aesar, Tewksbury, MA)] for 1 hr, stained overnight with primary antibodies at 4° and then incubated with Alexa Fluor 488- or Alexa Fluor 555-labelled secondary antibodies for 1 hr. The coverslips were mounted with ProLong Diamond Antifade Mountant with DAPI (Thermo Fisher Scientific). Images were taken on an LSM 800 scanning confocal microscope (Zeiss, Oberkochen, Germany). Differential interference contrast images (DIC) were included to capture the cell morphology.

Enzyme-linked immunosorbent assay (ELISA)

The levels of IFN-α, IFN-β, and IFN-λ1 and IFN-λ2/3 protein in culture supernatants were measured using VeriKine-HS Human IFN-α All Subtype ELISA Kit (PBL Assay Science, Piscataway, NJ, USA), VeriKine-HS Human IFN-Beta Serum ELISA Kit (PBL Assay Science), and Human IFN-λ1 ELISA Kit (Thermo Scientific) and the DIY Human IFN-λ2/3 (IL-28A/B) ELISA kits (PBL Assay Science, Piscataway, NJ), respectively, according to the manufacturers' protocols. The minimum detectable dose for IFN-α, IFN-β, IFN-λ1 and IFN-λ2/3 is 1.95, 2.3, 15.6 and 125 pg/ml, respectively.

Statistical analysis

Results were representative of at least three independent experiments. The values were expressed as mean and SD of individual samples. Statistical significance was determined by Student's *t*-test using the GraphPad Prism 7

(GraphPad, San Diego, CA). A $P < 0.05$ was considered a significant difference between the experimental groups.

Results

DNA-triggered Ku70 translocation and IFN production in different cell types

Human Ku70, as a DNA repair protein, is endogenously and dominantly expressed in the nucleus of the cells. We previously reported that Ku70 translocates from the nucleus to the cytoplasm upon transfection with DNA in HEK cells.[13] Utilizing confocal microscopy, we compared the translocation of Ku70 in HEK, RD and HeLa cells after transfection with DNA. The confocal images clearly indicated that Ku70 (red) mainly existed in the nucleus of untreated HEK, RD and HeLa cells (Figure 1A–C). Consistent with our previously observation,[13] six hours after MFP488-labelled DNA (green) transfection, Ku70 was mostly localized in the cytoplasm of HEK or RD cells (Figure 1A,B). However, Ku70 remained in the nucleus of HeLa cells (Figure 1C). To precisely quantify the translocation, we captured the images with multiple cells of the view and then calculated the percentage of cells containing cytoplasmic Ku70 with at least 200 cells were counted. All the images used for the percentage calculation are presented in Figure S1a–c. The percentage of cells with Ku70 cytoplasmic localization in HEK, RD and HeLa cells is shown in Figure 1D, over 80% cells with cytoplasmic Ku70 was observed in DNA-transfected HEK or RD cells. However, there is no significant difference between untreated and DNA-transfected HeLa cells (Figure 1D).

Along with the localization analysis of Ku70 after DNA transfection, IFN-λ1 induction was evaluated by real-time RT-PCR and ELISA using RNA cell lysate collected at 24 hr after DNA transfection and cell culture supernatants harvested at 48 hr after DNA transfection, respectively. The result showed that transfection with DNA highly induced IFN-λ1 production in HEK and RD cells (Figure 1E,F). However, IFN-λ1 was barely induced in DNA-transfected HeLa cells, which was consistent with

our previous observations (Figure 1E,F).[14,31] Meanwhile, we also measured DNA transfection-trigged IFN-α, IFN-β, IFN-λ2, IFN-λ3 and IFN-λ4 in HEK cells based on the availability of probes or ELISA kits. The result is shown in Figure S2a,b. The data indicated that IFN-λ1 was predominately induced in DNA-transfected HEK cells compared with the induction of IFN-α, IFN-β, IFN-λ2, IFN-λ3 and IFN-λ4. So, we will mainly characterize the induction of IFN-λ1 in the following experiments.

To confirm whether RNA transfection induces the translocation of Ku70, the localization of Ku70 was evaluated in MFP488-labelled poly (I:C)-transfected HEK cells. The images suggested that RNA transfection does not trigger the translocation of Ku70 from the nucleus to the cytoplasm (Figure 1A). The percentage of cells with cytoplasmic Ku70 is 15.95%, which is similar to 18.70% of cells with Ku70 cytoplasmic localization in untreated HEK cells (Figure S1a). So, the translocation of Ku70 is triggered by a DNA, but not RNA, transfection.

Based on those observations, it was reasonable to hypothesize that the translocation of Ku70 is correlated with the IFN-λ1 production. However, it was not clear whether Ku70 translocation is initiated by the transfected DNA or triggered by the induced IFN-λ1. To determine the role of IFN-λ1 on translocation, we treated HEK cells with different concentrations of recombinant IFN-λ1; then, we evaluated the localization of Ku70 using confocal microscopy (Figure S3). First, we determined the dose of IFN-λ1 treatment in HEK cells by checking the induction of one of the IFN-stimulated genes (ISGs). The binding between IFN-λ1 and its receptors (IL-10Rβ and IFN-λR1) leads to a signalling cascade, which is ISG activation. The best studied ISGs are the 2′,5′-oligo-adenylate synthetase (2′, 5′-OAS), the protein kinase R (PKR) and the MX genes. In contrast to 2′, 5′-OAS and PKR, MX expression is stimulated exclusively by IFN-α/β or IFN-λ.[32] We therefore used MX1 gene expression as a surrogate for IFN-λ1-mediated activity. As shown in Figure S3a, MX1 expression was highly induced by IFN-λ1 treatment at concentrations of 50 ng/ml and 500 ng/ml. Thus, we used the concentration of 500 ng/ml to treat

Figure 1. DNA-triggered Ku70 translocation and IFN-λ1 induction in different cell types. The localization of Ku70 was visualized under confocal microscope in (A) HEK, (B) RD and (C) HeLa cells with or without MFP488-labelled DNA/poly(I:C) transfection. Cells were grown on 15mm coverslip-inserted 12-well cell culture plates and transfected with or without MFP488-labelled DNA/poly(I:C), then fixed and stained with anti-Ku70 (red) antibody at 6 hr after nucleotide acid transfection. Nuclei were visualized by DAPI (blue). Cell morphology was observed with DIC (grey) setting. Original magnification was ×40. Scale bar: 10 μm. Isotype IgG control staining was included for Ku70 (red) channel. (D) Cells treated as in (A, B, C) were qualitatively examined to assess staining of Ku70 (red) in the nucleus or cytoplasm. Cells showing Ku70 cytoplasmic staining were counted and expressed as a percentage of total number of cells. At least 200 cells were counted per sample. The images used for the calculation are shown in Figure S1a–c. (E) Cells were seeded in 6-well cell culture plates, and further transfected with linearized DNA. Relative IFN-λ1 mRNA expression was measured by real-time RT-PCR at 24 hr after transfection, and the gene expression level for each cell type was compared with its untreated condition. (F) The cell culture supernatants were collected at 48 hr after DNA transfection, and the protein expression levels of IFN-λ1 were measured by ELISA assay. **$P < 0.01$, ***$P < 0.001$, and ns which represents not significantly difference (Student's t-test) are indicated in the figure where IFN-λ1 expression for each cell type was compared with its untreated condition.

(A)

(B)

(C)
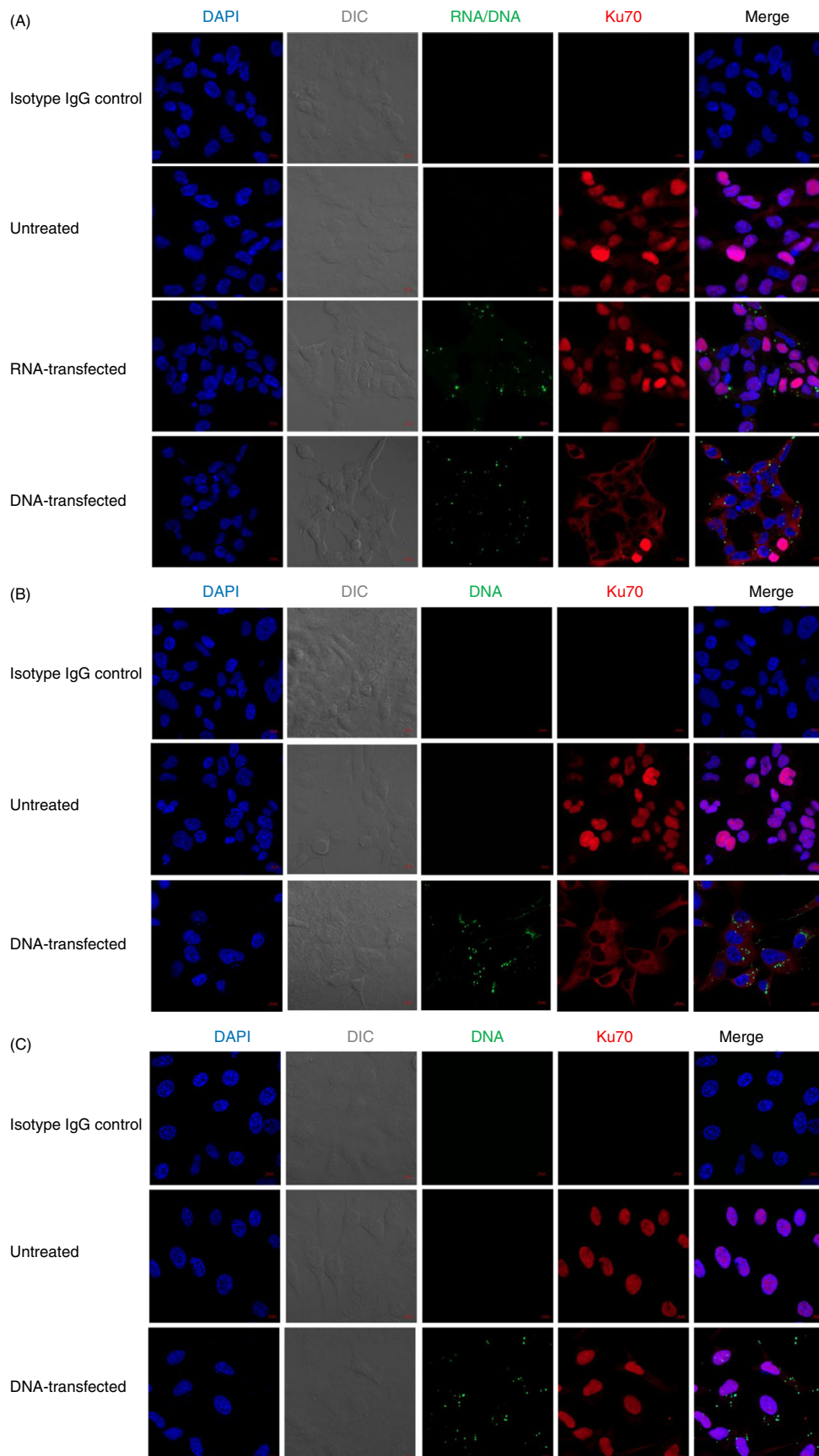
cells and then observed whether the translocation of Ku70 occurs. The result indicated that Ku70 (green) retained in the nucleus of the cells even in the presence of IFN-λ1 treatment, suggesting that induced IFN-λ1 has no significant role in inducing Ku70 translocation (Figure S3b). The event of Ku70 translocation may be caused earlier, and then, IFN-λ1 induction is prompted later.

Ku70 and Ku80 form a heterodimer called Ku protein, which is well known for its role in repairing DNA double-strand breaks by non-homologous end joining (NHEJ).[33] So, we are curious about the localization of Ku80, while Ku70 undergoes a translocation from the nucleus to the cytoplasm. Confocal images, as shown in Figure S4, indicated that both Ku70 (red) and Ku80 (green) mostly colocalized in the nucleus of unstimulated HEK cells. Upon transfection with DNA, both Ku70 (red) and Ku80 (green) mainly localized in the cytoplasm of the cells. These data indicated that together with Ku70, Ku80 also translocated from the nucleus to the cytoplasm when the cells were stimulated with DNA transfection.

Different HSV-1 virus strain infection-induced Ku70 translocation and IFN production

We further investigated whether infection by herpes simplex virus (HSV)-1, a DNA virus, triggers the translocation of Ku70 and induces IFN-λ1 in HEK cells. Two different strains of HSV-1 (MacIntyre and McKrae) were used in the study. The virus infection was confirmed by staining the cells using anti-HSV-1 antibody as described in Materials and methods (Figure 2A). The data indicated that the infection of HSV-1 McKrae strain induced remarkable cell morphology changes at 16 hr post-infection compared with uninfected cells. The infected cells aggregated together, and the expression of HSV-1 viral protein (in green) was mainly presented in the cytoplasm or membrane but not in the nucleus. The localization of Ku70 was mostly in the cytoplasm of the McKrae-infected cells (Figure 2A). About 91.02% of the infected cells demonstrated that Ku70 located in the cytoplasm

(Figure 2B, Figure S5). In contrast, compared with untreated cells, there is no notable morphology changes in the MacIntyre strain-infected cells, and the expression of HSV-1 viral protein was mainly existed in the nucleus. Ku70 mainly localized in the nucleus of the infected cells (Figure 2A); 14.85% of MacIntyre-infected cells contained cytoplasmic Ku70, which is similar to the percentage of uninfected cells (22.76%) (Figure 2B, Figure S5).

The expression of IFN-λ1 gene and protein levels were measured at 24 hr after virus infection using real-time PCR and ELISA assay, respectively. The result indicated that the infection of HSV-1 McKrae but not MacIntyre strain induced significant amounts of IFN-λ1 gene expression and protein expression levels (Figure 2C,D). The results consistently support the hypothesis that Ku70 translocation from the nucleus to the cytoplasm is a required step for DNA-stimulated IFN-λ1 induction.
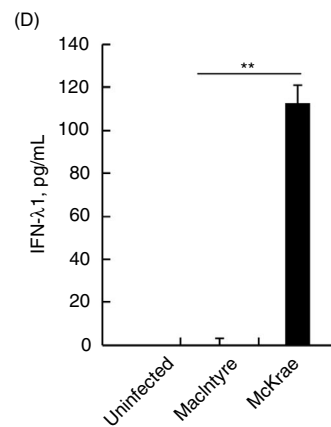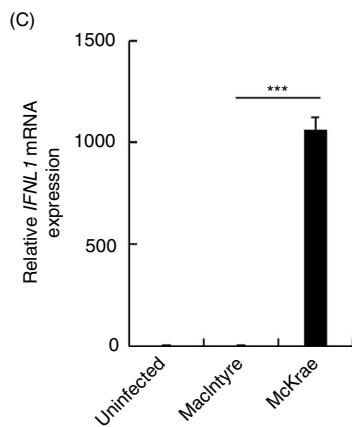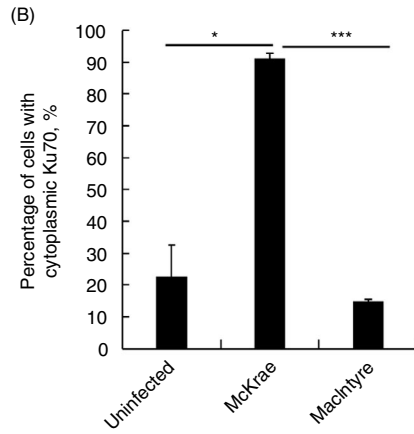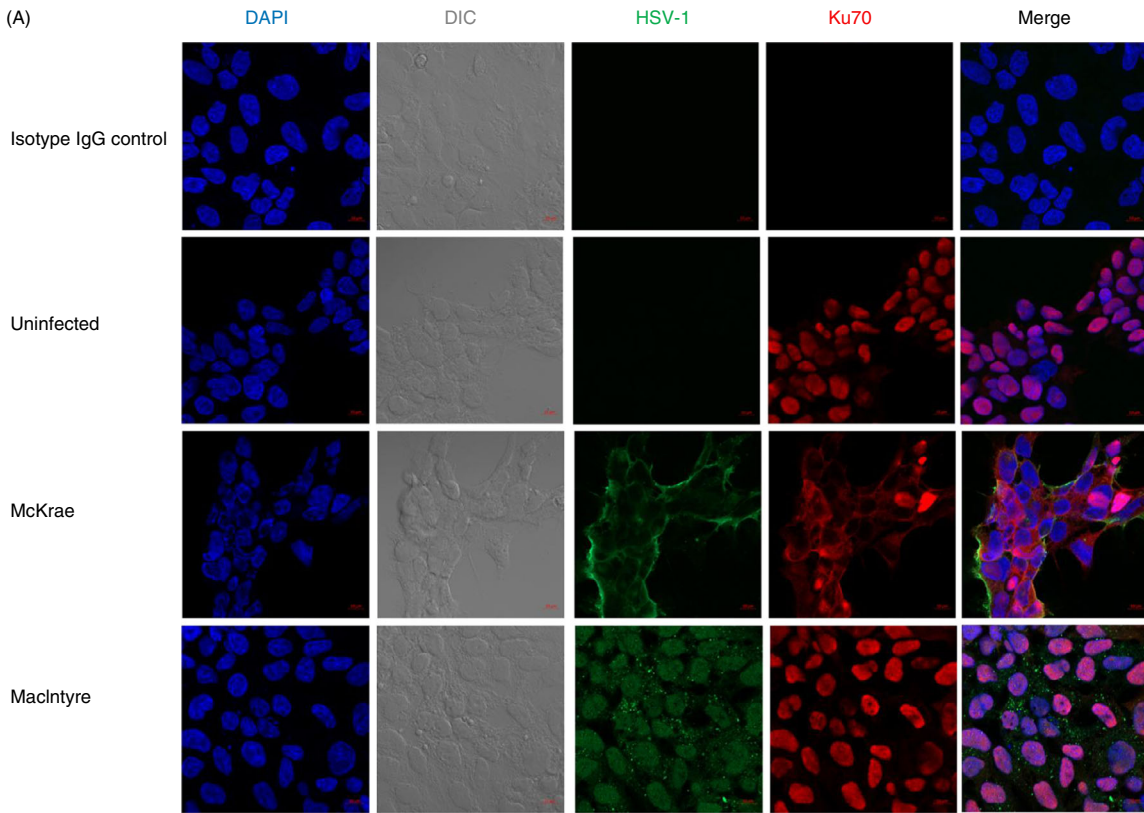
The cytoplasmic translocation of Ku70 is an early event in DNA-mediated IFN-λ1 induction pathway

To characterize a kinetics of the cytoplasmic translocation of Ku70, the accumulation of cytosolic Ku70 was measured by Western blot. The cytosolic fraction was extracted at 1, 3, 6, 18 and 24 hr after DNA transfection. The band intensity of Ku70 was normalized by the intensity of β-actin using Fiji–ImageJ. The normalized value is indicated in Figure 3A. The result indicated that the accumulation of Ku70 was initiated right after DNA transfection and was peaked at 6 hr after DNA transfection.

We next determined the impact of leptomycin B (LMB), an inhibitor of nuclear export, on Ku70 translocation and DNA-mediated IFN-λ1 induction. It has been demonstrated that LMB is able to accumulate the nuclear proteins, such as IRAK-1 and NLRC5,[34,35] in the nucleus. CRM1 (exportin 1) is identified as the cellular target of LMB and considered an evolutionarily conserved receptor for the NLS of proteins.[36] HEK cells were treated with LMB (5 nM) at 1 hr after DNA transfection. Confocal

---

Figure 2. Different HSV-1 virus strain infection-induced Ku70 translocation and IFN-λ1 induction in HEK cells. (A) The localization of Ku70 was visualized under confocal microscope in HEK cells infected with HSV-1 MacIntyre or McKrae strain at MOI of 1. Cells were grown on 15 mm coverslip-inserted 12-well cell culture plates and infected with or without HSV-1 MacIntyre or McKrae strain. The cells were then fixed at 16 hr after infection and stained with anti-Ku70 (red) antibody and anti-HSV-1 (green) antibody. Nuclei were visualized by DAPI (blue). Cell morphology was observed with DIC (grey) setting. Original magnification was ×40. Scale bar: 10 μm. Isotype IgG control staining was included for HSV-1 (green) and Ku70 (red) channels. (B) Cells treated as in (A) were qualitatively examined to assess staining of Ku70 (red) in the nucleus or cytoplasm. Cells showing Ku70 cytoplasmic staining were counted and expressed as a percentage of total number of cells. At least 200 cells were counted per sample. The images used for the calculation are shown in Figure S5. (C) Cells were seeded in 6-well cell culture plates, and further infected with HSV-1 virus strain MacIntyre or McKrae at MOI of 1. Relative IFN-α, IFN-β and IFN-λ1 gene expression was measured by real-time RT-PCR at 24 h after infection, and the gene expression level was compared with uninfected cells. (D) The cell supernatants were collected at 24 hr after virus infection, and the protein expression of IFN-α, IFN-β and IFN-λ1 was measured by ELISA assay. *P < 0.05, **P < 0.01, ***P < 0.001 (Student's t-test) are indicated in the figure where the IFN-λ1 expression level was compared between HSV-1 McKrae virus infection and MacIntyre virus infection.
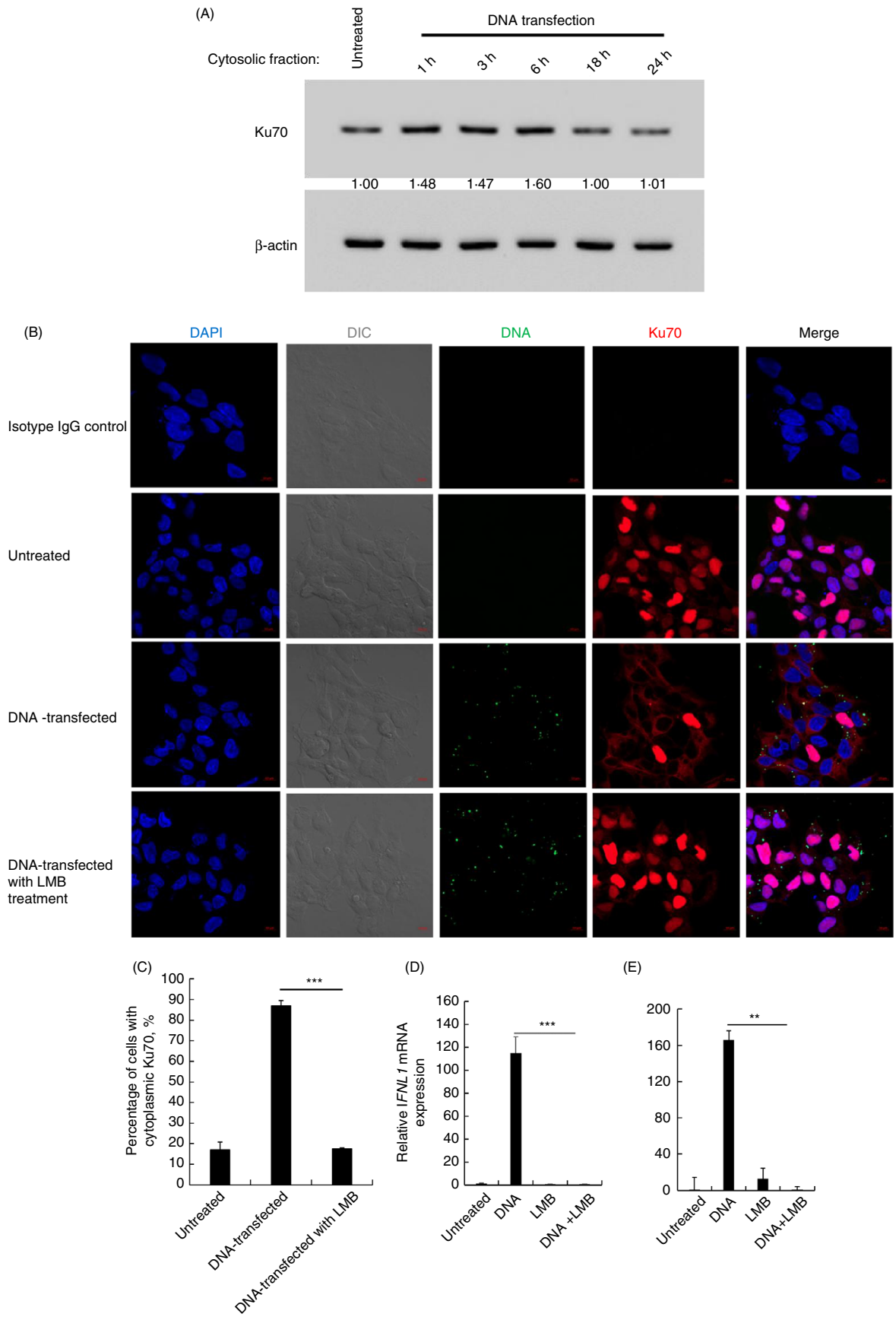
(A)

(B)

(C)

(D)

Figure 3. The cytoplasmic translocation of Ku70 is an early event in DNA-mediated IFN-λ1 induction pathway. (A) HEK cells were seeded in 6-well cell culture plates and then transfected with linearized DNA. Then, cytosolic factions were prepared at 1, 3, 6, 18 and 24 hr after transfection, followed by Western blot using anti-Ku70 antibody. β-Actin is included as a loading control. The intensity of the band for Ku70 was normalized by the intensity of β-actin, and the value for Ku70/β-actin is indicated in the image, which is analysed by Fiji–ImageJ. (B) HEK cells were seeded on 15 mm coverslip-inserted 12-well cell culture plates and transfected with or without MFP488-labelled DNA. The cells were then incubated with 5 nM LMB at 1 hr after DNA transfection. Then, six hours later, the cells were fixed and stained with anti-Ku70 (red) antibody. Nuclei were visualized by DAPI (blue). Cell morphology was observed with DIC (grey) setting. Original magnification was ×40. Scale bar: 10 μm. Isotype IgG control staining was included for Ku70 (red) channel. (B) Cells treated as in (A) were qualitatively examined to assess staining of Ku70 (red) in the nucleus or cytoplasm. Cells showing Ku70 cytoplasmic staining were counted and expressed as a percentage of total number of cells. At least 200 cells were counted per sample. The images used for the calculation are shown in Figure S6. (D) HEK cells were transfected with DNA and then treated 5 nM LMB at 1 hr after transfection. Twenty-four hours after DNA transfection, the cells were collected for RNA extraction. Relative IFN-λ1 mRNA expression was measured by real-time RT-PCR, and the gene expression level was compared with untreated cells. (E) The cell supernatants were collected 48 hr after DNA transfection for ELISA assay to measure IFN-λ1 protein expression. **$P < 0.01$ and ***$P < 0.001$ (Student's t-test) are indicated in the figure where the gene expression level was compared between with or without LMB treatment.

images showed that, in the presence of LMB, the localization of Ku70 (red) mainly presented in the nucleus of the cells (Figure 3B). Cytoplasmic Ku70 was detected in 87.02% of DNA-transfected cells in the absence of LMB, while in the presence of LMB, only 17.44% of the DNA-transfected cells contained cytoplasmic Ku70 (Figure 3C and Figure S6).

We also assessed the impact of LMB on the IFN induction. The results indicated that LMB significantly inhibited DNA-induced IFN-λ1 production (Figure 3D,E). These results illustrated that blocking of nuclear export suppressed both the translocation of Ku70 and the production of IFNs, which provides further evidence that Ku70 translocation from the nucleus to the cytoplasm is an essential and initial step for DNA/Ku70-induced innate immune response.

Acetylation regulates Ku70/DNA-mediated IFN-λ1 induction

Several studies reported that cytoplasmic Ku70 via acetylation regulates the activity and stability of apoptosis-related proteins.[37–42] As a nuclear protein, Ku70 encodes a bipartite type of NLS. The Ku70 NLS contains five lysines (K539, K542, K544, K553 and K556) that were identified as targets for acetylation *in vivo*.[18,29] Lysine acetylation in the cytoplasm drives and coordinates key events such as cytoskeleton dynamics, intracellular trafficking, vesicle fusion, metabolism and stress response.[43,44] We hypothesized that acetylation of the five lysine residues in the Ku70 NLS acts as a switch controlling the translocation of Ku70 from the nucleus to the cytoplasm.[37–42] It is reported that the basic amino acids between Lys553 and Lys556 are needed for nuclear translocation.[45] Thus, we constructed acetylation-mimicking double mutations at NLS of Ku70 named Ku70 K553Q/K556Q. Then, the localization of mutant Ku70 was observed under confocal microscope. The construction map for wild-type Ku70 (Ku70 WT) and mutant Ku70 (Ku70 MT) is shown in

Figure 4A. The confocal images demonstrated that Ku70 WT (green) distributed in the nucleus of the cells (Figure 4B). However, Ku70 MT was expressed in the cytoplasm of the cells (Figure 4B). Therefore, we demonstrated that recombinant Ku70 mutants in which specific NLS lysine residues were substituted with glutamine to mimic acetylation exhibited reduced translocation to the nucleus. To quantitatively demonstrate the difference in Ku70 localization, a western blot was performed using the cytosolic fraction of the Ku70 WT- or Ku70 MT-overexpressed HEK cells. The band intensity of anti-Flag was normalized by the intensity of β-actin using Fiji–ImageJ. The result indicated that the expression level of cytoplasmic protein of Ku70 MT was 10.9-fold higher than that of Ku70 WT. (Figure 4C).

We next assessed the capability of mutant Ku70 to activate IFN-λ1 promoter using the IFN-λ1 reporter assay.[13,14] The result demonstrated that Ku70 MT highly increased the IFN-λ1 promoter activity compared with Ku70 WT (Figure 4D).

A level of protein acetylation is correlated with the result from a dynamic equilibrium between the activity of acetyltransferases and the opposing deacetylases. Histone deacetylases (HDACs) also regulate deacetylation of multiple non-histone protein substrates and impact their functions by altering their activity, cellular location and protein–protein interactions. More than 50 non-histone proteins, such as p53, Ku70, have been reported to be the substrates of HDACs.[46] So, we treated cells with trichostatin A (TSA), an inhibitor that is sensitive to Class I/II deacetylases, and then measured the impact of deacetylation inhibitor on DNA via Ku70-mediated IFN-λ1 induction. The result indicated that treatment with TSA dose-dependently increased IFN-λ1 production (Figure 4E). These results further supported that acetylation modulates Ku70-mediated DNA sensing. To further delineate a correlation between cytoplasmic Ku70 and IFN induction, the accumulated cytosolic Ku70 was quantified by Western blot using the TSA-treated cytosolic fractions. The
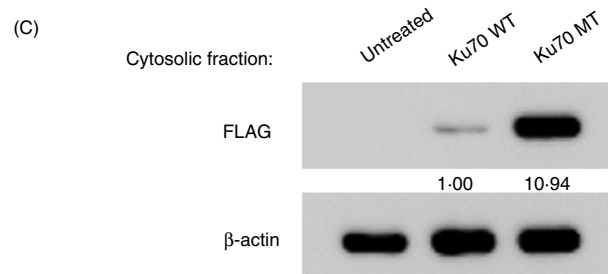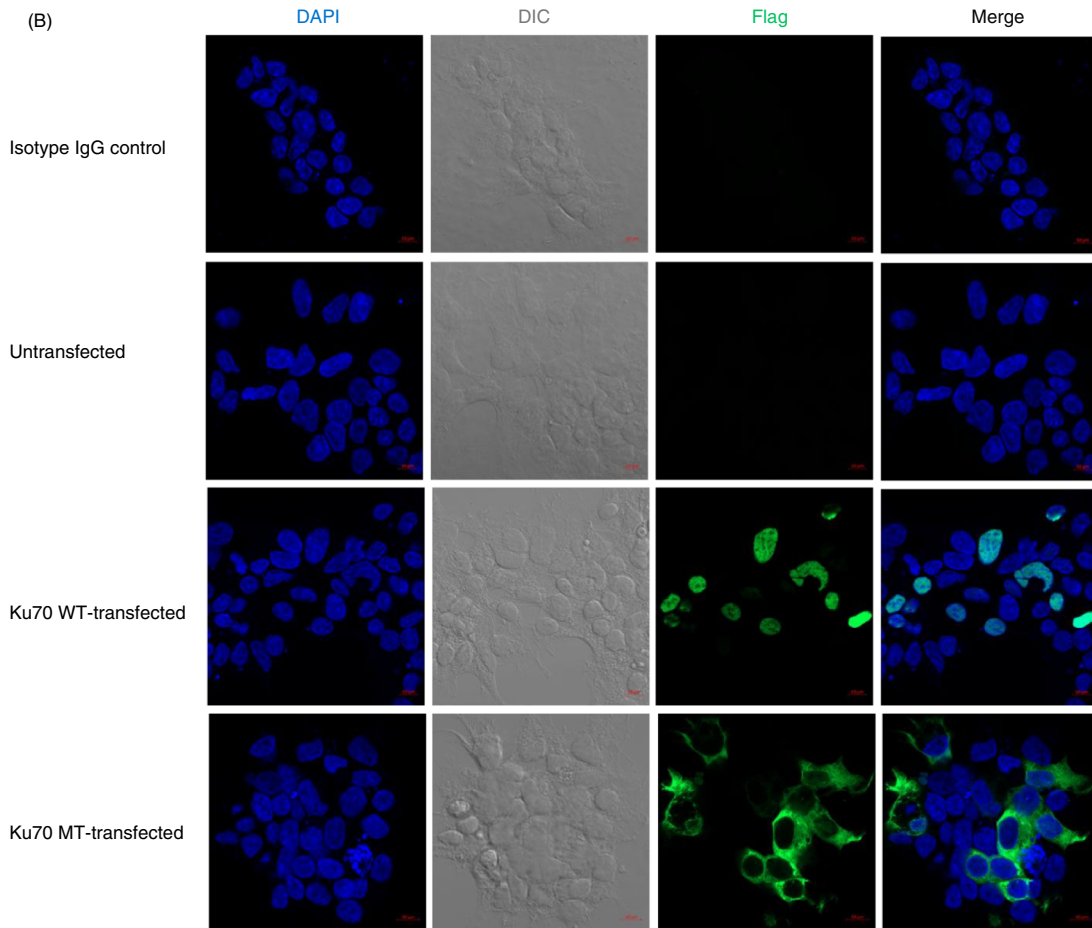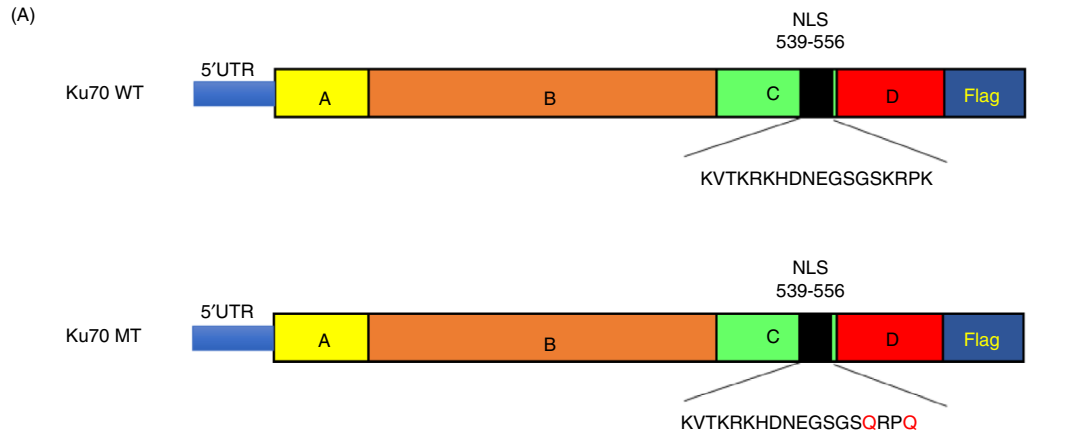
(A)

(B)

(C)

Figure 4. Acetylation regulates Ku70/DNA-mediated IFN-λ1 induction. (A) The diagram of FLAG-tagged wild-type Ku70 (Ku70 WT) and FLAG-tagged acetylation-mimicking mutation of lysine residues 553 and 556 of Ku70 (Ku70 MT). (B) The intracellular distribution of wild-type Ku70 or mutant Ku70 is demonstrated by confocal microscopy. HEK cells were seeded on 15 mm coverslip-inserted 12-well cell culture plates and transfected with FLAG-tagged wild-type Ku70 or FLAG-tagged mutant Ku70. Thirty-six hours later, the cells were fixed and stained with anti-FLAG (green) antibody. Nuclei were visualized by DAPI (blue). Cell morphology was observed with DIC (grey) setting. Original magnification was ×40. Scale bar: 10 μm. Isotype IgG control staining for FLAG (green) channel is included. (C) HEK cells were overexpressed by Ku70 WT or Ku70 MT vectors. Then, cytosolic factions were prepared followed by Western blot using anti-Flag antibody. β-Actin is included as a loading control. The intensity of the band for Flag was normalized by the intensity of β-actin, and the value for Flag-Ku70/β-actin is indicated in the image, which is analysed by Fiji–ImageJ. (D) The comparison of the capability of Ku70 to activate IFN-λ1 promoter activity between wild-type Ku70 (Ku70 WT) and mutant Ku70 (Ku70 MT) with acetylation-mimicking mutation of lysine residues 553 and 556. 293T cells were cotransfected with IFN-λ1 reporter plasmid (pGL4-IFN-λ1), Renilla luciferase plasmid (pRL-TK) and STING expression vector together with wild-type Ku70 or mutant Ku70 expression vectors. Cells were then stimulated with linearized plasmid DNA on day 3. On day 4, cells were collected for luciferase assay. **$P < 0.01$ (Student's t-test) is indicated in the figure where relative IFN-λ1 promoter luciferase activity was compared between Ku70 WT and Ku70 MT. (E, F) HEK cells were treated with TSA at the indicated concentrations (0, 10, 30, 100 and 300 nM). One day after, the cells were then transfected with DNA. (E) Twenty-four hours after DNA transfection, the cells were collected for RNA extraction. Relative IFN-λ1 mRNA expression was measured by real-time RT-PCR, and the gene expression level was compared with untreated cells. (F) The cytosolic factions were prepared at 6 hr after DNA transfection and then followed by Western blot using anti-Flag antibody. β-Actin is included as a loading control. The intensity of the band for Ku70 was normalized by the intensity of β-actin, and the value for Ku70/β-actin was indicated in the image, which is analysed by Fiji–ImageJ. (G) A correlation plot between the accumulation of cytosolic Ku70 and DNA-mediated relative *IFNL1* induction (trendline and R-squared value is indicated). [Correction added on 23 April 2021, after first online publication: In Figure 4 (A) second panel, the label has been changed from 'Ku70 WT' to 'Ku70 MT' in this version.]

band intensity of Ku70 was normalized by that of β-actin using Fiji–ImageJ, the values of Ku70/β-actin are indicated in Figure 4F. Compared with untreated cells, TSA dose-dependently increased the accumulation of cytosolic Ku70. Taken together, TSA increases the accumulation of cytoplasmic Ku70 and therefore enhances DNA-mediated IFN-λ1 induction. A positive correlation was found between the accumulation of cytosolic Ku70 and DNA-mediated IFN-λ1 induction (Figure 4G, $R^2 = 0.9577$).

Discussion

The current study demonstrated that the translocation of Ku70 from the nucleus to the cytoplasm is an early and required event in Ku70/DNA-mediated IFN-λ1 induction and acetylation plays an essential role in modulating ku70's cytosolic DNA sensing by promoting cytosolic accumulation of Ku70. We diagrammed a summary of our current and previous findings[13,14] about DNA or DNA virus via Ku70-mediated IFN-λ1 signalling pathway in Figure 5. Ku70 undergoes a translocation from the nucleus to the cytoplasm, the cytoplasmic Ku70 recognizes cytosolic viral DNA or other forms of DNA followed by interacting with STING and activating the downstream TBK1-IRFs signalling pathway. Enhancing acetylation facilitates accumulation of cytoplasmic Ku70 and then enhances the activity of Ku70-mediated cytosolic DNA sensing. At this moment, how transfection with DNA or infection with DNA virus primes or triggers the translocation remains unclear. One hypothesis is a change in a dynamic equilibrium between nuclear and cytosolic Ku70 protein upon DNA binding. When cytosolic Ku70 binds and forms a complex with cytoplasmic DNA, the interaction may disrupt the equilibrium between the cytosolic and the nucleus Ku70 and drive the translocation of Ku70 from the nucleus to the cytosol. IFI16, another DNA sensor protein, reported as not only cytosolic but also nuclear DNA sensor, and the sensing capabilities depend on the localization of IFI16.[47–49] Our finding is in line with the finding for IFI16. However, it remains unknown whether Ku70 also serves as a nuclear DNA sensor such as IFI16. A recent study reported that Ku70 is involved in HIV or another lentivirus (HTLV-1) integration in the nucleus.[50–52] Therefore, understanding the mechanism of Ku70 translocation may also provide a new target for antiviral therapy.

It is known that Ku70 forms a heterodimer complex with Ku80, and we also demonstrated in the current study that Ku80 translocated with Ku70 from the nucleus to the cytoplasm, suggesting that Ku70 and Ku80 may translocate as the heterodimer. It is reported that both Ku70 and Ku80 are highly unstable when expressed individually[53] and loss of one of the Ku subunits results in a significant decrease in the steady-state level of the other.[54–56] Therefore, it is difficult for us to further precisely clarify a counterpart dependency in the translocation of Ku70 using the current approaches and systems. We believe that further studies to elucidate the molecular mechanisms of the translocation of Ku protein will lead to a better understanding of the physiological functions of Ku protein.

In our previous work, we demonstrated that transiently knockdown of Ku70, but not Ku80, decreases IFN-λ1 induction.[14] To define a role of Ku70 or Ku80 in the IFN response, we had utilized IFN-λ1 promoter reporter assay by overexpression of each protein. And the results consistently indicated that overexpression of Ku70 enhanced the activity of IFN-λ1 promoter. However,
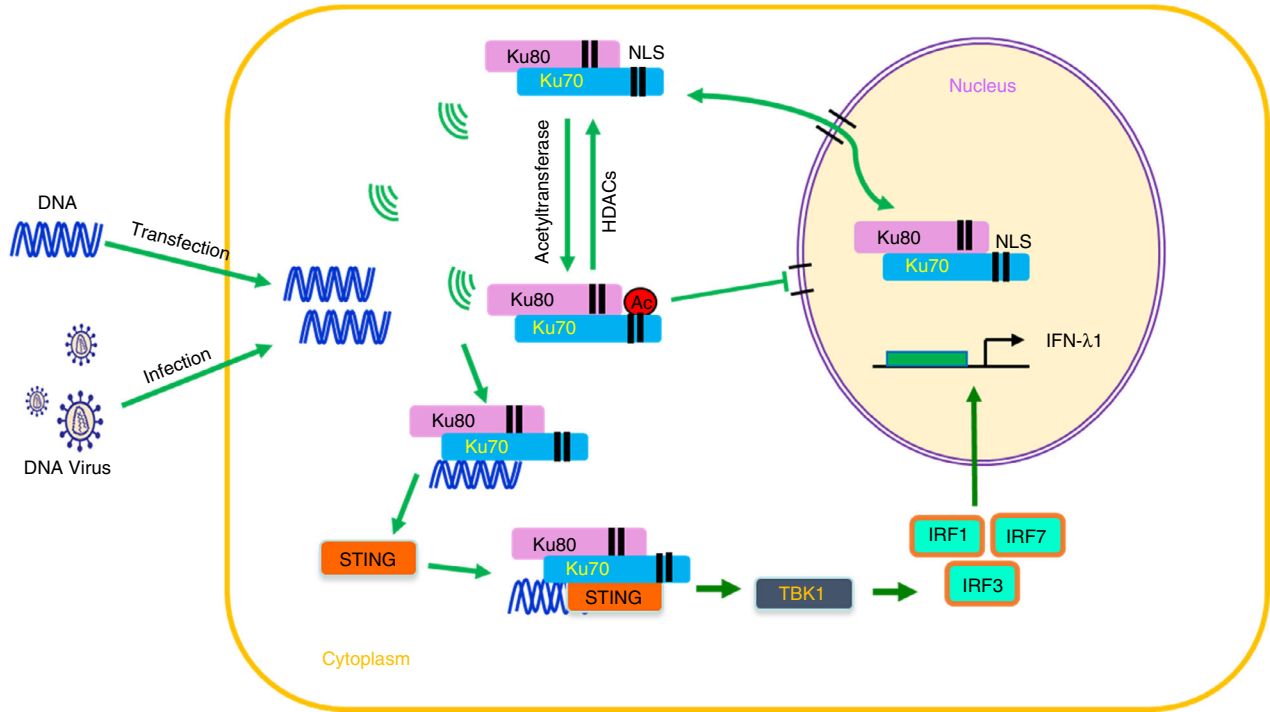
Figure 5. Working model for the cytosolic DNA-sensing activity of Ku70. Ku70 undergoes a translocation from the nucleus to the cytoplasm to recognize cytosolic viral DNA or other form of DNA followed by interacting with STING and activating the downstream IFN-λ1 signalling pathway. Acetylation modulates DNA-mediated Ku70-dependent IFN-λ1 induction. Ku80 colocalizes with Ku70 during Ku70 translocation from the nucleus to the cytoplasm, but not directly involving in Ku70's cytosolic DNA-sensing activity.

overexpression of Ku80 had no impact on IFN-λ1 promoter activation,[13] suggesting that Ku80 may not be directly involved in the DNA sensing or the activation of downstream signalling.

In the current study, we demonstrated that HSV-1 virus infection-induced Ku70 translocation and IFN-λ1 induction were consistently caused in an HSV-1 strain-dependent manner. Ku70 translocation occurred in the cells infected by HSV-1 McKrae strain, but not MacIntyre strain. Herpes viruses are a large family of DNA viruses. After a virus binds to the cell surface, viral entry is caused by either endocytosis or direct fusion of virion membrane with the plasma membrane of host cells.[57] The productive infection is initiated by efficient and rapid transport of the incoming capsids across the cytosol to the nucleus. This step involves a microtubule-dependent pathway. Finally, the viral DNA genomes are released into the nucleoplasm.[57] However, Horan *et al.* reported that a capsid of HSV-1 strain 17 is ubiquitinated in the cytoplasm of cells and degraded via the ubiquitin–proteasome pathway. This degradation subsequently leads viral DNA to be immediately sensed by DNA sensors.[58] The study demonstrated that some of HSV-1 strains may release DNA into the cytosol. Therefore, a question of whether the localization of viral DNA in HSV-1 McKrae-infected cells differs from that in MacIntyre-infected cells remains unclear. And our confocal images demonstrate a difference in the localization of HSV-1 viral protein between HSV-1 MacIntyre- and

McKrae-infected cells. Additionally, the finding of our study also implied that the virus strain dependency may be associated with a difference in the acetylation level of Ku70. To demonstrate a profile of DNA virus-dependent acetylation on Ku70 and a correlation between the acetylation and the IFN-λ1 induction may delineate the mechanism of the viral strain-dependent immune response. To precisely define the mechanism underlying the strain dependency in the IFN induction and Ku70 translocation, we recently completed full-length viral DNA sequences of two strains[59,60] and a comparative study is currently underway. Deschamps and Kalamyoki reported that HSV-1 strain 17 UL46 suppresses STING-mediated IFN-β and ISG expression in HEL cells, a human erythroleukaemia cell line.[61] Of interest, our DNA sequence analysis revealed that HSV-1 virus strain McKrae encodes an identical sequence of UL46 with HSV-1 strain 17, and our further study showed that both McKrae and 17 strain induced innate immune response, especially IFN-α induction in primary human macrophages (Figure S7); thus, UL46 may differentially function in the regulation of IFN induction in a host cell-dependent manner. More evidences are needed to elucidate mechanism of the innate immune activation via virus strain dependency, which may provide a new insight into the mechanism of immune escape of HSV infection and its subtype dependency.

We also confirmed that acetylation at NLS of Ku70 is 'a toggle switch' for localization of Ku70 as other

reported[45] and involved in its DNA-sensing activity. The loss of nuclear accumulation of Ku70 K553Q/K556Q is due to decreased interaction with the Impα/Impβ complex, and thus, the acetylation of two specific Ku70 lysine residues, K553 and K556, modulates nuclear import.[45] These findings further supported that translocation of Ku70 to the nucleus is controlled by the acetylation of specific lysine residues in the NLS. Protein acetylation levels *in vivo* are the result of a dynamic equilibrium between the activity of acetyltransferases and the opposing deacetylases.[42,47] As we confirmed in the current study, increasing the acetylation by TSA treatment, Ku70-mediated IFN-λ1 induction was dose-dependently enhanced through promoting the cytoplasmic accumulation of Ku70. We observed that Ku70 differentially localized in different cell types. Therefore, we speculate that the diversity in the Ku70 localization may be modulated by level of uncharacterized cell type-specific acetylation enzymes. Augmentation of cytoplasmic localization of Ku70 may maximize immune response against DNA virus infection. Acetylation may provide a simple and elegant mechanism for fine-tuning Ku70 distribution for its DNA-sensing function or other localization-dependent activities.

DNA is a powerful immunostimulatory agent in many contexts. Under the context of DNA virus infection, the innate immune system has to be able to detect DNA from pathogens in order to induce a strong antiviral innate immune response.[62] It is reported that DNA vaccination relies on DNA sensing to invoke a powerful innate immune response that, in turn, assists the adaptive response.[63] DNA can also act as a damage-associated molecular pattern (DAMP), accelerating inflammatory responses following its release from dying or damaged cells directly contributing to the pathogenesis of various diseases such as atherosclerosis[64] and deep vein thrombosis.[65] Deregulation of immune signalling may lead to autoinflammation and autoimmunity in some instances.[66]

DNA-induced innate immune response is not only restricted an induction of IFN-α or IFN-β, but also included an induction of type III IFNs (IFN-λs).[67–70] IFN-λs are key antiviral cytokines, directly performing an antiviral immune response at epithelial surfaces in the early stages of viral infection, and that these cytokines also skew the balance of Th1 and Th2 cells to Th1 phenotype.[71] Type III IFN signalling through its receptors serves as a positive feedback loop, increasing IFN-λ1 induction will provide benefit for antitumour activity.[72] Therefore, it is also important to regulate type III innate immune response to fight viral infections, autoimmune diseases and tumours.

In the current study, we demonstrated Ku70's cytoplasmic translocation as an early and required event for DNA via Ku70-mediated type III IFN response. We reported for the first time that enhancing acetylation promotes cytoplasmic translocation of Ku70 and facilitates DNA-mediated IFN-λ1 induction. The finding has important implications for ongoing efforts to inhibit the antiviral response to treat autoimmune diseases, and for the possibility of harnessing this pathway to enhance immune responses to tumours and for understanding of induction of the beneficial cytokine storm under DNA vaccination.

Acknowledgments

Conflict of interest

The authors declare no competing interest.

Author contributions

H.S. and Q.C. performed experiments. H.S. and T.I. designed, discussed and interpreted the data. T.I. constructed Ku70 K553Q/K556Q mutant. H.S. and T.I. wrote the manuscript.

Data availability statement

The data support the finding of this study are available from the corresponding author upon reasonable request.

References

1 Medzhitov R, Janeway C. Innate Immunity. *N Engl J Med* 2000; **343**:338–44.

2 Akira S, Uematsu S, Takeuchi O. Pathogen recognition and innate immunity. *Cell* 2006; **124**:783–801.

3 Mitsutoshi Y, Takashi F. Recognition of viral nucleic acids in innate immunity. *Rev Med Virol* 2010; **20**:4–22.

4 Paludan Søren R, Bowie AG. Immune sensing of DNA. *Immunity* 2013; **38**:870–80.

5 Thompson MR, Kaminski JJ, Kurt-Jones EA, Fitzgerald KA. Pattern recognition receptors and the innate immune response to viral infection. *Viruses* 2011; **3**:920–40.

6 Yoneyama M, Fujita T. Recognition of viral nucleic acids in innate immunity. *Rev Med Virol* 2010; **20**:4–22.

7 Takaoka A. DAI (DLM-1/ZBP1) is a cytosolic DNA sensor and an activator of innate immune response. *Nature* 2007; **448**:501–5.

8 Chiu YH, Macmillan JB, Chen ZJ. RNA polymerase III detects cytosolic dna and induces type I interferons through the RIG-I pathway. *Cell* 2009; **138**:576–91.

9 Unterholzner L, Keating SE, Baran M, Horan KA, Jensen SB, Sharma S, *et al*. IFI16 is an innate immune sensor for intracellular DNA. *Nat Immunol* 2010; **11**:997–1004.

10 Kim T, Pazhoor S, Bao M, Zhang Z, Hanabuchi S, Facchinetti V, *et al*. Aspartate-glutamate-alanine-histidine box motif (DEAH)/RNA helicase A helicases sense microbial DNA in human plasmacytoid dendritic cells. *Proc Natl Acad Sci USA* 2010; **107**:15181–6.

11 Sun L, Wu J, Du F, Chen XG, Chen ZJ. Cyclic GMP-AMP synthase is a cytosolic DNA sensor that activates the Type I Interferon Pathway. *Science* 2013; **339**:786–91.

12 Xia P, Wang S, Gao P, Gao G, Fan Z. DNA sensor cGAS-mediated immune recognition. *Protein Cell* 2016; **7**:777–91.

13 Sui H, Zhou M, Imamichi H, Jiao X, Sherman BT, Lane HC, et al. STING is an essential mediator of the Ku70-mediated production of IFN-λ1 in response to exogenous DNA. *Science Signaling* 2017; **10**:eaah5054.

14 Zhang X, Brann TW, Zhou M, Yang J, Oguariri RM, Lidie KB, et al. Cutting edge: Ku70 is a novel cytosolic DNA sensor that induces type III rather than type I IFN. *J Immunol* 2011; **186**:4541–5.

15 Rivera-Calzada A, Spagnolo L, Pearl LH, Llorca O. Structural model of full-length human Ku70–Ku80 heterodimer and its recognition of DNA and DNA-PKcs. *EMBO Rep* 2007; **8**:56–62.

16 Critchlow SE, Jackson SP. DNA end-joining: from yeast to man. *Trends Biochem Sci* 1998; **23**:394–8.

17 Mimori T, Hardin JA, Steitz JA. Characterization of the DNA-binding protein antigen Ku recognized by autoantibodies from patients with rheumatic disorders. *J Biol Chem* 1986; **261**:2274–4.

18 Cohen HY, Lavu S, Bitterman KJ, Hekking B, Imahiyerobo TA, Miller C, et al. Acetylation of the C Terminus of Ku70 by CBP and PCAF controls Bax-mediated apoptosis. *Mol Cell* 2004; **13**:627–38.

19 Subramanian C, Opipari AW, Bian X, Castle VP, Kwok RPS. Ku70 acetylation mediates neuroblastoma cell death induced by histone deacetylase inhibitors. *Proc Natl Acad Sci USA* 2005; **102**:4842–7.

20 Mazumder S, Plesca D, Kinter M, Almasan A. Interaction of a Cyclin E fragment with Ku70 regulates Bax-mediated. *Apoptosis* 2007; **27**:3511–20.

21 Hada M, Subramanian C, Andrews PC, Kwok RP. Cytosolic Ku70 regulates Bax-mediated cell death. *Tumour Biol* 2016; **37**:13903–14.

22 Ferguson BJ, Mansur DS, Peters NE, Ren H, Smith GL. DNA-PK is a DNA sensor for IRF-3-dependent innate immunity. *Elife* 2012; **1**:e00047.

23 Li Y, Wu Y, Zheng X, Cong J, Liu Y, Li J, et al. Cytoplasm-translocated Ku70/80 complex sensing of HBV DNA induces hepatitis-associated chemokine secretion. *Front Immunol* 2016; **7**:569.

24 Wang J, Kang L, Song D, Liu L, Yang S, Ma L, et al. Ku70 senses HTLV-1 DNA and modulates HTLV-1 replication. *J Immunol* 2017; **199**:2475–82.

25 Krebber H, Silver PA. Directing proteins to nucleus by fusion to nuclear localization signal tags. In: Thorner J, Emr SD, Abelson JN, eds. Methods in Enzymology. Cambridge, MA: Academic Press, 2000: 283–96.

26 Görlich D, Mattaj IW. Nucleocytoplasmic transport. *Science* 1996; **271**:1513–9.

27 Freitas N, Cunha C. Mechanisms and signals for the nuclear import of proteins. *Curr Genomics* 2009; **10**:550–7.

28 Schwoebel ED, Ho TH, Moore MS. The mechanism of inhibition of Ran-dependent nuclear transport by cellular ATP depletion. *J Cell Biol* 2002; **157**:963–74.

29 Koike M, Ikuta T, Miyasaka T, Shiomi T. The nuclear localization signal of the human Ku70 is a variant bipartite type recognized by the two components of nuclear pore-targeting complex. *Exp Cell Res* 1999; **250**:401–13.

30 Blaho JA, Morton ER, Yedowitz JC. Herpes simplex virus: propagation, quantification, and storage. *Curr Protoc Microbiol* 2006; 14E.1.1–23.

31 Sui H, Zhou M, Chen Q, Lane HC, Imamichi T. siRNA enhances DNA-mediated interferon lambda-1 response through crosstalk between RIG-I and IFI16 signalling pathway. *Nucleic Acids Res* 2014; **42**:583–98.

32 Holzinger D, Jorns C, Stertz S, Boisson-Dupuis S, Thimme R, Weidmann M, et al. Induction of MxA gene expression by influenza A virus requires type I or type III interferon signaling. *J Virol* 2007; **81**:7776–85.

33 Liang F, Romanienko PJ, Weaver DT, Jeggo PA, Jasin M. Chromosomal double-strand break repair in Ku80-deficient cells. *Proc Natl Acad Sci USA* 1996; **93**:8929–33.

34 Benko S, Magalhaes JG, Philpott DJ, Girardin SE. NLRC5 limits the activation of inflammatory pathways. *J Immunol* 2010; **185**:1681–91.

35 Liu G, Park Y-J, Abraham E. Interleukin-1 receptor-associated kinase (IRAK) -1-mediated NF-κB activation requires cytosolic and nuclear activity. *FASEB J* 2008; **22**:2285–96.

36 Kudo N, Matsumori N, Taoka H, Fujiwara D, Schreiner EP, Wolff B, et al. Leptomycin B inactivates CRM1/exportin 1 by covalent modification at a cysteine residue in the central conserved region. *Proc Natl Acad Sci USA* 1999; **96**:9112–7.

37 Lee SJ, Jang H, Park C. Maspin increases Ku70 acetylation and Bax-mediated cell death in cancer cells. *Int J Mol Med* 2012; **29**:225–30.

38 Tao NN, Ren JH, Tang H, Ran LK, Zhou HZ, Liu B, et al. Deacetylation of Ku70 by SIRT6 attenuates Bax-mediated apoptosis in hepatocellular carcinoma. *Biochem Biophys Res Commun* 2017; **485**:713–9.

39 Subramanian C, Jarzembowski JA, Halsey SM, Kuick R, Opipari AW Jr, Castle VP, et al. CLU blocks HDACI-mediated killing of neuroblastoma. *Tumour Biol* 2011; **32**:285–94.

40 Roth M, Wang Z, Chen WY. SIRT1 and LSD1 competitively regulate KU70 functions in DNA repair and mutation acquisition in cancer cells. *Oncotarget* 2016; **7**:50195–214.

41 Sundaresan NR, Samant SA, Pillai VB, Rajamohan SB, Gupta MP. SIRT3 is a stress-responsive deacetylase in cardiomyocytes that protects cells from stress-mediated cell death by deacetylation of Ku70. *Mol Cell Biol* 2008; **28**:6384–401.

42 Gong P, Li K, Li Y, Liu D, Zhao L, Jing Y. HDAC and Ku70 axis- an effective target for apoptosis induction by a new 2-cyano-3-oxo-1,9-dien glycyrrhetinic acid analogue. *Cell Death Dis* 2018; **9**:623.

43 Sadoul K, Wang J, Diagouraga B, Khochbin S. The tale of protein lysine acetylation in the cytoplasm. *J Biomed Biotechnol* 2011;2011:1–15.

44 Yang X-J, Seto E. Lysine acetylation: codified crosstalk with other posttranslational modifications. *Mol Cell* 2008; **31**:449–61.

45 Fujimoto H, Ikuta T, Koike A, Koike M. Acetylation of nuclear localization signal controls importin-mediated nuclear transport of Ku70. *bioRxiv* 2018.

46 Gong P, Wang Y, Jing Y. Apoptosis induction by histone deacetylase inhibitors in cancer cells: role of Ku70. *Int J Mol Sci* 2019; **20**:1601.

47 Ansari MA, Dutta S, Veettil MV, Dutta D, Iqbal J, Kumar B, et al. Herpesvirus genome recognition induced acetylation of nuclear IFI16 is essential for its cytoplasmic translocation, inflammasome and IFN-β responses. *PLoS Pathog* 2015; **11**:e1005019.

48 Dell'Oste V, Gatti D, Gugliesi F, De Andrea M, Bawadekar M, Lo Cigno I, et al. Innate nuclear sensor IFI16 translocates into the cytoplasm during the early stage of in vitro human cytomegalovirus infection and is entrapped in the egressing virions during the late stage. *J Virol* 2014; **88**:6970–82.

49 Li T, Diner BA, Chen J, Cristea IM. Acetylation modulates cellular distribution and DNA sensing ability of interferon-inducible protein IFI16. *Proc Natl Acad Sci USA* 2012; **109**(26):10558–63.

50 Knyazhanskaya E, Anisenko A, Shadrina O, Kalinina A, Zatsepin T, Zalevsky A, et al. NHEJ pathway is involved in post-integrational DNA repair due to Ku70 binding to HIV-1 integrase. *Retrovirology* 2019; **16**:30.

51 Zheng Y, Ao Z, Wang B, Jayappa KD, Yao X. Host protein Ku70 binds and protects HIV-1 integrase from proteasomal degradation and is required for HIV replication. *J Biol Chem* 2011; **286**:17722–35.

52 Anisenko AN, Knyazhanskaya ES, Zalevsky AO, Agapkina JY, Sizov AI, Zatsepin TS, et al. Characterization of HIV-1 integrase interaction with human Ku70 protein and initial implications for drug targeting. *Sci Rep* 2017; **7**:5649.

53 Satoh M, Wang J, Reeves WH. Role of free p70 (Ku) subunit in posttranslational stabilization of newly synthesized p80 during DNA-dependent protein kinase assembly. *Eur J Cell Biol* 1995; **66**:127–35.

54 Errami A, Smider V, Rathmell WK, He DM, Hendrickson EA, Zdzienicka MZ, et al. Ku86 defines the genetic defect and restores X-ray resistance and V(D)J recombination to complementation group 5 hamster cell mutants. *Mol Cell Biol* 1996; **16**:1519–26.

55 Singleton BK, Priestley A, Steingrimsdottir H, Gell D, Blunt T, Jackson SP, et al. Molecular and biochemical characterization of xrs mutants defective in Ku80. *Mol Cell Biol* 1997; **17**:1264–73.

56 Gu Y, Seidl KJ, Rathbun GA, Zhu C, Manis JP, van der Stoep N, et al. Growth retardation and leaky SCID phenotype of Ku70-deficient mice. *Immunity* 1997; **7**:653–65.

57 Pellett PE, Roizman B. The Family Herpesviridae: A Brief Introduction. In D.M. Knipe, P.M. Howley, D.E. Griffin, R.A. Lamb, M.A. Martin, B. Roizman, S.E. Straus, (Eds.), Fields Virology. (2, pp. 2479–2499). Philadelphia, PA: Lippincott Williams & Wilkins, 2007.

58 Horan KA, Hansen K, Jakobsen MR, Holm CK, Søby S, Unterholzner L, et al. Proteasomal degradation of herpes simplex virus capsids in macrophages releases DNA to the cytosol for recognition by DNA sensors. *J Immunol* 2013; **190**:2311–9.

59 Jiao X, Sui H, Lyons C, Tran B, Sherman BT, Imamichi T. Complete genome sequence of Herpes Simplex Virus 1 Strain MacIntyre. *Microbiol Resour Announc* 2019; **8**:e00895-19.

60 Jiao X, Sui H, Lyons C, Tran B, Sherman BT, Imamichi T. Complete genome sequence of Herpes Simplex Virus 1 Strain McKrae. *Microbiol Resour Announc* 2019; **8**:e00993-19.

61 Deschamps T, Kalamvoki M. Evasion of the STING DNA-sensing pathway by VP11/12 of Herpes Simplex Virus 1. *J Virol* 2017; **91**:e00535-17.

62 Federico S, Pozzetti L, Papa A, Carullo G, Gemma S, Butini S, et al. Modulation of the innate immune response by targeting toll-like receptors: a perspective on their agonists and antagonists. *J Med Chem* 2020; **63**:13466–513.

63 Ishii KJ. TANK-binding kinase-1 delineates innate and adaptive immune responses to DNA vaccines. *Nature* 2008; **451**:725–9.

64 Oka T, Hikoso S, Yamaguchi O, Taneike M, Takeda T, Tamai T, et al. Mitochondrial DNA that escapes from autophagy causes inflammation and heart failure. *Nature* 2012; **485**:251–5.

65 Brill A, Fuchs TA, Savchenko AS, Thomas GM, Martinod K, De Meyer SF, et al. Neutrophil extracellular traps promote deep vein thrombosis in mice. *J Thromb Haemost* 2012; **10**:136–44.

66 Rioux JD, Abbas AK. Paths to understanding the genetic basis of autoimmune disease. *Nature* 2005; **435**:584–9.

67 Ank N, Iversen MB, Bartholdy C, Staeheli P, Hartmann R, Jensen UB, *et al.* An important role for Type III Interferon (IFN-{lambda}/IL-28) in TLR-induced antiviral activity. *J Immunol* 2008; **180**:2474–85.

68 Ank N, Paludan SR. Type III IFNs: new layers of complexity in innate antiviral immunity. *BioFactors* 2009; **35**:82–7.

69 Ank N, West H, Bartholdy C, Eriksson K, Thomsen AR, Paludan SR. Lambda Interferon (IFN-λ), a Type III IFN, is induced by viruses and IFNs and displays potent antiviral activity against select virus infections in vivo. *J Virol* 2006; **80**:4501–9.

70 Bartlett NW, Buttigieg K, Kotenko SV, Smith GL. Murine interferon lambdas (type III interferons) exhibit potent antiviral activity in vivo in a poxvirus infection model. *J Gen Virol* 2005; **86**:1589–96.

71 Zhou JH, Wang YN, Chang QY, Ma P, Hu Y, Cao X. Type III interferons in viral infection and antiviral immunity. *Cell Physiol Biochem* 2018; **51**:173–85.

72 Chen J, Markelc B, Kaeppler J, Ogundipe VML, Cao Y, McKenna WG, *et al.* STING-dependent Interferon-λ1 induction in HT29 cells, a human colorectal cancer cell line, after gamma-radiation. *Int J Radiat Oncol Biol Phys* 2018; **101**:97–106.

Supporting Information

Additional Supporting Information may be found in the online version of this article:

Table S1. A list of antibodies used for western blot and immunofluorescence assays. The information about the catalog numbers, suppliers and clone numbers are provided.

Table S2. A list of Assay Identification Number for the FAM-MGB probes used in the real-time RT-PCR assay. All the probes were purchased from Thermo Fisher Scientific.

Figure S1. The merged confocal images to determine the percentage of cells containing cytoplasmic Ku70. The localization of Ku70 was visualized under confocal microscope. (a) HEK (b) RD and (c) HeLa cells were seeded on coverslip-inserted 12-well plates, and then were transfected with MFP488-labelled linearized DNA or MFP 488-labelled poly (I:C). Six hours later, the cells were fixed and stained with anti-Ku70 (red) antibody. Nuclei were visualized by DAPI (blue). Original magnification was ×40. Scale bar: 20 μm. The percentage of cells with cytoplasmic Ku70 was indicated. Total counted cell number is > 200.

Figure S2. DNA transfection-induced IFN-α, IFN-β, IFN-λ1, IFN-λ2, IFN-λ3 or IFN-λ4 production. HEK cells were treated with linearized DNA transfection, and (a) the relative *IFNA, IFNB, IFNL1, IFNL2, IFNL2/3* or *IFNL4* gene expression was measured by real-time RT-PCR at 24 hr after treatment. (b) The cell supernatants were collected at 48h after DNA transfection. The protein expression level of IFN-α, IFN-β, IFN-λ1 or IFN-λ2/3 was measured by ELISA assay.

Figure S3. IFN-λ1 treatment did not induce the translocation of Ku70 from the nucleus to the cytoplasm. (a) HEK cells were treated with different concentration of IFN-λ1. And relative MX1 gene expression was measured by real-time RT-PCR at 24 hr after treatment. The treatment with IFNα at 5 ng/ml was used as a positive control. (b) The localization of Ku70 was visualized under confocal microscope. HEK cells were seeded on coverslip-inserted 12-well plates, and then were incubated with 500 ng/ml of IFN-λ1. Twenty-four hours later the cells were fixed and stained with anti-Ku70 (red) antibody. Nuclei were visualized by DAPI (blue). Cell morphology was observed with DIC (grey) setting. Original magnification was ×40. Scale bar: 10 μm. The isotype IgG control was included for Ku70 channel.

Figure S4. The localization of Ku80 was visualized under confocal microscope. HEK cells were seeded on coverslip-inserted 12-well plates and transfected with or without DNA. Six hours later after DNA transfection, the cells were fixed and stained with anti-Ku70 (green), and anti-Ku80 (red) antibody. Nuclei were visualized by DAPI (blue). Cell morphology was observed with DIC (grey) setting. Original magnification was ×40. Scale bar: 5 μm. The isotype IgG control staining was included for Ku70 and Ku80 channels.

Figure S5. The merged confocal images to determine the percentage of cells containing cytoplasmic Ku70. The localization of Ku70 was visualized under confocal microscope. HEK cells were seeded on coverslip-inserted 12-well plates, and then were infected with HSV-1 McKrae strain or MacIntyre strain at MOI of 1. Sixteen hours later the cells were fixed and stained with anti-Ku70 (red) and anti-HSV-1 (green) antibodies. Nuclei were visualized by DAPI (blue). Original magnification was ×40. Scale bar: 20 μm. The percentage of cells with cytoplasmic Ku70 was indicated. Total counted cell number is > 200.

Figure S6. The merged confocal images to determine the percentage of cells containing cytoplasmic Ku70. The localization of Ku70 was visualized under confocal microscope. HEK cells were seeded on coverslip-inserted 12-well plates, and then were transfected with MFP488-labelled DNA (green) with or without LMB treatment at 1 hr after DNA transfection. 6 hr after DNA transfection, the cells were fixed and stained with anti-Ku70 (red) antibody. Nuclei were visualized by DAPI (blue). Original magnification was ×40. Scale bar: 20 μm. The percentage of cells with cytoplasmic Ku70 was indicated. Total counted cell number is > 200.

Figure S7. Different HSV-1 virus strain infection-induced IFN induction in macrophages. Human primary macrophages were infected by HSV-1 virus strain MacIntyre, McKrae and 17 at MOI of 1·0. The cells were harvested for total RNA extraction at 24 hr after infection. Relative (a) *IFNL1*, (b) *IFNB*, (c) *IFNA8*, (d) *IFNA13* and (e) *IFNA14* mRNA expression was measured by real-time RT-PCR, and the gene expression level was compared to uninfected cells.